Original Article

Institution of MECHANICAL ENGINEERS

Journal of MECHANICAL ENGINEERING SCIENCE

Proc IMechE Part C:
J Mechanical Engineering Science
0(0) 1–12

DOI: 10.1177/0954406217729421
journals.sagepub.com/home/pic
SAGE

Porosity-dependent vibration and dynamic stability of compositionally gradient nanofilms using nonlocal strain gradient theory

Mohammad Reza Barati

Abstract

Porosity-dependent free vibration and dynamic stability of functionally graded nanofilms are studied according to the nonlocal strain gradient theory. Two-scale coefficients are considered to incorporate both nonlocality and strain gradient impacts. The nanofilm is subjected to in-plane hygro-thermal and harmonic mechanical loads. Uniform dispersion of porosities is considered according to a power-law model for functionally graded materials. Galerkin's approach is employed to obtain the vibration frequencies as well as stability regions. One can see that stability regions and vibration frequencies of a functionally graded nanofilm are significantly affected by static load parameter, dynamic load parameter, porosities, moisture change, temperature change, and elastic substrate nonlocal strain gradient coefficients.

Keywords

Porous nanofilm, nonlocal strain gradient theory, classical plate theory, hygro-thermal environment, dynamic stability

Date received: 27 March 2017; accepted: 7 August 2017

Introduction

It is well-known that the mechanical performance of functionally graded (FG) structures is significantly influenced by the change in moisture and temperature fields. An increment in the value of moisture and temperature results in lower stiffness of FG structures. Since FG structures are constructed from two phases with graded properties from ceramic to metal phase, they are different from other composite materials under combined moisture and temperature effects called hygro-thermal loading. Actually, material composition of FG structures has a remarkable impact on their behavior in hygro-thermal environment.[1–8]

Nanostructures constructed from FG materials[9–12] have been applied as structural components in nano-electro-mechanical systems (NEMs).[13–15] For theoretical modeling and analysis of nanostructures, it is important to use a nonclassical elasticity theory containing scale parameters. Actually, these scale parameters can introduce size-dependency of nanostructures. One of these nonclassical theories is nonlocal elasticity theory proposed by Eringen,[16,17] which introduces a nonlocal stress field to describe wide range interaction between atoms. This theory has efficiently employed by many researchers to examine static and dynamic characteristics of nanostructures.[18–35] Nonlocal elasticity theory is also applied for the analysis of vibration,[36–42] buckling,[43–45] and wave propagation[46–48] of FG nanostructures. In all of afore-mentioned articles, only stiffness reduction mechanism due to nonlocality is considered.

It is well-known that in nonlocal modeling of nanostructures, strain gradient effects have been discarded. Thus, only stiffness-softening effects are reported and stiffness enhancement due to strain gradients is not observed.[49] A general nonlocal strain gradient theory (NSGT) can be introduced, while its efficiency in the wave propagation analysis of nanobeams is examined by Lim et al.[50] This theory is also employed by Li et al.[51] for the wave propagation analysis of FG nanobeams. Li et al.[52] explored buckling behavior of FG nanobeams under axial mechanical load using NSGT. In another work, Farajpour et al.[53] performed buckling analysis of nanoscale homogenous plates employing NSGT.

Aerospace Engineering Department & Center of Excellence in Computational Aerospace, Amirkabir University of Technology, Tehran, Iran

Corresponding author:
Mohammad Reza Barati, Aerospace Engineering Department & Center of Excellence in Computational Aerospace, Amirkabir University of Technology, 424, Hafez Avenue, Tehran, Iran.
Emails: mrb.barati@ymail.com; mrb.barati@aut.ac.ir

Barati and Shahverdi[54] examined hygro-thermal vibration analysis of graded double-refined-nanoplate systems using hybrid nonlocal stress–strain gradient theory. Also, Barati[55] explored wave dispersion behavior of FG nanobeams with the effect of porosities and nonlocal strain gradient theory. Therefore, it is of great importance to analyze the dynamic behavior of FG nanoplates via NSGT.

Free vibration and dynamic stability of porous FG nanofilms are investigated according to nonlocal strain gradient theory. Two-scale coefficients are considered to incorporate both nonlocality and strain gradient impacts. The nanofilm is subjected to in-plane hygro-thermal and harmonic mechanical loads. Uniform dispersion of porosities are considered according to power-law model for FG materials. Galerkin's approach is employed to obtain the vibration frequencies as well as stability regions. One can see that stability regions and vibration frequencies of a FG nanofilm are significantly affected by static load parameter, dynamic load parameter, porosities, moisture change, temperature change, elastic substrate nonlocal strain gradient coefficients. Obtained results can be used for further investigations on nanofilms incorporating nonlocal and microstructure-dependent strain gradient theories.

Nonlocal strain gradient nanoplate model

The proposed nonlocal strain gradient theory[54] takes into account both nonlocal stress field and the strain gradient effects by introducing two-scale parameters. This theory defines the stress field as

$$\sigma_{ij} = \sigma_{ij}^{(0)} - \nabla \sigma_{ij}^{(1)} \tag{1}$$

where the stresses $\sigma_{ij}^{(0)}$ and $\sigma_{ij}^{(1)}$ are corresponding to strain ε_{ij} and strain gradient $\nabla\varepsilon_{ij}$, respectively as

$$\sigma_{ij}^{(0)} = \int_V C_{ijkl}\alpha_0(x, x', e_0a)\varepsilon'_{kl}(x')dx' \tag{2a}$$

$$\sigma_{ij}^{(1)} = l^2 \int_V C_{ijkl}\alpha_1(x, x', e_1a)\nabla\varepsilon'_{kl}(x')dx' \tag{2b}$$

where C_{ijkl} are the elastic coefficients and e_0a and e_1a capture the nonlocal effects and l captures the strain gradient effects. When the nonlocal functions $\alpha_0(x, x', e_0a)$ and $\alpha_1(x, x', e_1a)$ satisfy the developed conditions by Eringen, the constitutive relation of nonlocal strain gradient theory has the following form

$$\begin{aligned}&\left[1-(e_1a)^2\nabla^2\right]\left[1-(e_0a)^2\nabla^2\right]\sigma_{ij}\\&= C_{ijkl}\left[1-(e_1a)^2\nabla^2\right]\varepsilon_{kl} - C_{ijkl}\,l^2\left[1-(e_0a)^2\nabla^2\right]\nabla^2\varepsilon_{kl}\end{aligned} \tag{3}$$

where ∇^2 denotes the Laplacian operator. Considering $e_1 = e_0 = e$, the general constitutive relation in equation (3) becomes

$$\left[1-(ea)^2\nabla^2\right]\sigma_{ij} = C_{ijkl}\left[1-l^2\nabla^2\right]\varepsilon_{kl} \tag{4}$$

To consider the hygro-thermal effects equation (4) can be written as[55]

$$\left[1-(ea)^2\nabla^2\right]\sigma_{ij} = C_{ijkl}\left[1-l^2\nabla^2\right](\varepsilon_{kl} - \gamma_{ij}T - \beta_{ij}C) \tag{5}$$

where γ_{ij} and β_{ij} are thermal and moisture expansion coefficients, respectively.

FG plate model based on neutral surface position

Consider a rectangular (a × b) porous nanofilm of uniform thickness h made of FGM as shown in Figure 1. An FG material can be specified by the variation in the volume fractions. Due to this variation, neutral axis of FG nanofilm may not coincide with its mid-surface, which leads to bending-extension coupling. By using neutral axis, this coupling is eliminated. Based on the modified power-law model, Young' modulus E, density ρ, thermal expansion coefficient γ, and moisture expansion coefficient β are described as

$$E(z) = (E_c - E_m)\left(\frac{z}{h}+\frac{1}{2}\right)^p + E_m - \frac{\xi}{2}(E_c + E_m) \tag{6a}$$

$$\rho(z) = (\rho_c - \rho_m)\left(\frac{z}{h}+\frac{1}{2}\right)^p + \rho_m - \frac{\xi}{2}(\rho_c + \rho_m) \tag{6b}$$

$$\gamma(z) = (\gamma_c - \gamma_m)\left(\frac{z}{h}+\frac{1}{2}\right)^p + \gamma_m - \frac{\xi}{2}(\gamma_c + \gamma_m) \tag{6c}$$

$$\beta(z) = (\beta_c - \beta_m)\left(\frac{z}{h}+\frac{1}{2}\right)^p + \beta_m - \frac{\xi}{2}(\beta_c + \beta_m) \tag{6d}$$

where c and m denote the material properties of ceramic and metal phases, respectively and p is inhomogeneity or power-law index. Also, ξ is the porosity volume fraction. The displacement field according to the classical plate model considering exact position of neutral surface can be expressed by

$$u_1(x, y, z, t) = u(x, y, t) - (z - z^*)\frac{\partial w}{\partial x} \tag{7a}$$

$$u_2(x, y, z, t) = v(x, y, t) - (z - z^*)\frac{\partial w}{\partial y} \tag{7b}$$

$$u_3(x, y, z, t) = w(x, y, t) \tag{7c}$$

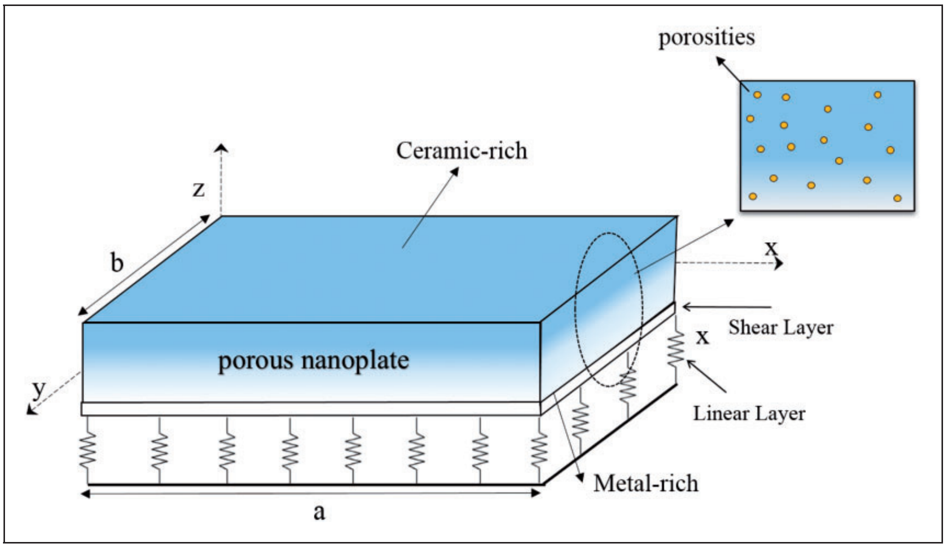

Figure 1. Configuration of nanoporous inhomogeneous nanoplate on elastic substrate.

where

$$z^* = \frac{\int_{-h/2}^{h/2} E(z)\, z dz}{\int_{-h/2}^{h/2} E(z)\, dz} \tag{8}$$

Also, u and v are in-plane displacements. According to the present plate theory, the nonzero strains are obtained as

$$\begin{aligned} \varepsilon_x &= \frac{\partial u}{\partial x} - (z - z^*)\frac{\partial^2 w}{\partial x^2} \\ \varepsilon_y &= \frac{\partial v}{\partial y} - (z - z^*)\frac{\partial^2 w}{\partial y^2} \\ \gamma_{xy} &= \frac{\partial u}{\partial y} + \frac{\partial v}{\partial x} - 2(z - z^*)\frac{\partial^2 w}{\partial x \partial y} \end{aligned} \tag{9}$$

Also, the extended Hamilton's principle express that

$$\int_0^t \delta(U - T + V)\, dt = 0 \tag{10}$$

Here, U is strain energy, T is kinetic energy, and V is work done by external forces. The first variation of the strain energy can be calculated as

$$\begin{aligned} \delta U = \int_V \Big(&\sigma_{xx}\delta\,\varepsilon_{xx} + \sigma_{xx}^{(1)}\delta\nabla\,\varepsilon_{xx} + \sigma_{yy}\delta\,\varepsilon_{yy} \\ &+ \sigma_{yy}^{(1)}\delta\nabla\,\varepsilon_{yy} + \sigma_{xy}\delta\,\gamma_{xy} + \sigma_{xy}^{(1)}\delta\nabla\,\gamma_{xy}\Big)\, \mathrm{d}V \end{aligned} \tag{11}$$

where σ are the components of the stress tensor and ε are the components of the strain tensor.

Substituting equations (8) and (10) into equation (12) yields

$$\begin{aligned} \delta U = \int_0^a \int_0^b \Bigg[& N_{xx}\left[\frac{\partial \delta u}{\partial x} + \frac{\partial w}{\partial x}\frac{\partial \delta w}{\partial x}\right] - M_{xx}^b \frac{\partial^2 \delta w}{\partial x^2} \\ & + N_{yy}\left[\frac{\partial \delta v}{\partial y} + \frac{\partial w}{\partial y}\frac{\partial \delta w}{\partial y}\right] - M_{yy}^b \frac{\partial^2 \delta w}{\partial y^2} \\ & + N_{xy}\left(\frac{\partial \delta u}{\partial y} + \frac{\partial \delta v}{\partial x} + \frac{\partial w}{\partial x}\frac{\partial \delta w}{\partial y} + \frac{\partial w}{\partial y}\frac{\partial \delta w}{\partial x}\right) \\ & - 2M_{xy}^b \frac{\partial^2 \delta w}{\partial x \partial y}\Bigg] dydx \end{aligned} \tag{12}$$

in which

$$\begin{aligned} N_{xx} &= \int_{-h/2}^{h/2} (\sigma_{xx}^0 - \nabla\sigma_{xx}^{(1)}) dz = N_{xx}^{(0)} - \nabla N_{xx}^{(1)} \\ N_{xy} &= \int_{-h/2}^{h/2} (\sigma_{xy}^0 - \nabla\sigma_{xy}^{(1)}) dz = N_{xy}^{(0)} - \nabla N_{xy}^{(1)} \\ N_{yy} &= \int_{-h/2}^{h/2} (\sigma_{yy}^0 - \nabla\sigma_{yy}^{(1)}) dz = N_{yy}^{(0)} - \nabla N_{yy}^{(1)} \\ M_{xx}^b &= \int_{-h/2}^{h/2} z(\sigma_{xx}^0 - \nabla\sigma_{xx}^{(1)}) dz = M_{xx}^{b(0)} - \nabla M_{xx}^{b(1)} \\ M_{yy}^b &= \int_{-h/2}^{h/2} z(\sigma_{yy}^0 - \nabla\sigma_{yy}^{(1)}) dz = M_{yy}^{b(0)} - \nabla M_{yy}^{b(1)} \\ M_{xy}^b &= \int_{-h/2}^{h/2} z(\sigma_{xy}^0 - \nabla\sigma_{xy}^{(1)}) dz = M_{xy}^{b(0)} - \nabla M_{xy}^{b(1)} \end{aligned} \tag{13}$$

where

$$\begin{aligned} N_{ij}^{(0)} &= \int_{-h/2}^{h/2} (\sigma_{ij}^{(0)}) dz, \quad N_{ij}^{(1)} = \int_{-h/2}^{h/2} (\sigma_{ij}^{(1)}) dz \\ M_{ij}^{b(0)} &= \int_{-h/2}^{h/2} z(\sigma_{ij}^{b(0)}) dz, \quad M_{ij}^{b(1)} = \int_{-h/2}^{h/2} z(\sigma_{ij}^{b(1)}) dz \end{aligned} \tag{14}$$

in which ($ij = xx,\ xy,\ yy$). The first variation of the work done by applied forces can be written as

$$\begin{aligned}\delta V = \int_0^a \int_0^b \Bigg(& N_x^0 \frac{\partial w}{\partial x}\frac{\partial \delta w}{\partial x} + N_y^0 \frac{\partial w}{\partial y}\frac{\partial \delta w}{\partial y} \\ & + 2\delta N_{xy}^0 \frac{\partial w}{\partial x}\frac{\partial w}{\partial y} - k_w w \delta w \\ & + k_p \left(\frac{\partial w}{\partial x}\frac{\partial \delta w}{\partial x} + \frac{\partial w}{\partial y}\frac{\partial \delta w}{\partial y} \right) \Bigg) dy dx \end{aligned} \tag{15}$$

where N_x^0, N_y^0, N_{xy}^0 are in-plane applied loads; k_w and k_p are Winkler and Pasternak constants. The first variation of the kinetic energy can be written in the following form

$$\begin{aligned}\delta K = \int_0^a \int_0^b \Bigg[& I_0 \left(\frac{\partial u}{\partial t}\frac{\partial \delta u}{\partial t} + \frac{\partial v}{\partial t}\frac{\partial \delta v}{\partial t} + \frac{\partial w}{\partial t}\frac{\partial \delta w}{\partial t} \right) \\ & - I_1 \left(\frac{\partial u}{\partial t}\frac{\partial \delta w}{\partial x \partial t} + \frac{\partial w}{\partial x \partial t}\frac{\partial \delta u}{\partial t} + \frac{\partial v}{\partial t}\frac{\partial \delta w}{\partial y \partial t} + \frac{\partial w}{\partial y \partial t}\frac{\partial \delta v}{\partial t} \right) \\ & + I_2 \left(\frac{\partial w}{\partial x \partial t}\frac{\partial \delta w}{\partial x \partial t} + \frac{\partial w}{\partial y \partial t}\frac{\partial \delta w}{\partial y \partial t} \right) \Bigg] dy dx \end{aligned} \tag{16}$$

in which

$$(I_0, I_1, I_2) = \int_{-h/2}^{h/2} (1, z - z^*, (z - z^*)^2) \rho(z) dz \tag{17}$$

By inserting equations (12) to (16) into equation (10) and setting the coefficients of $\delta u, \delta v, \delta w$ to zero, the following Euler–Lagrange equations can be obtained

$$\frac{\partial N_x}{\partial x} + \frac{\partial N_{xy}}{\partial y} = I_0 \frac{\partial^2 u}{\partial t^2} - I_1 \frac{\partial^3 w}{\partial x \partial t^2} \tag{18}$$

$$\frac{\partial N_{xy}}{\partial x} + \frac{\partial N_y}{\partial y} = I_0 \frac{\partial^2 v}{\partial t^2} - I_1 \frac{\partial^3 w}{\partial y \partial t^2} \tag{19}$$

$$\begin{aligned} & \frac{\partial^2 M_x^b}{\partial x^2} + 2\frac{\partial^2 M_{xy}^b}{\partial x \partial y} + \frac{\partial^2 M_y^b}{\partial y^2} \\ & \quad - (N^T + N^H)\nabla^2 w - k_w w + k_p \nabla^2 w \\ & = I_0 \frac{\partial^2 w}{\partial t^2} + I_1 \left(\frac{\partial^3 u}{\partial x \partial t^2} + \frac{\partial^3 v}{\partial y \partial t^2} \right) - I_2 \nabla^2 \left(\frac{\partial^2 w}{\partial t^2} \right) \end{aligned} \tag{20}$$

where $N_x^0 = N_y^0 = N^T + N^H, N_{xy}^0 = 0$ and hygro-thermal resultant can be expressed by

$$\begin{aligned} N^T &= \int_{-h/2}^{h/2} \frac{E(z)}{1-v} \gamma(z) (T - T_0)\, dz \\ N^H &= \int_{-h/2}^{h/2} \frac{E(z)}{1-v} \beta(z) (C - C_0)\, dz \end{aligned} \tag{21}$$

in which $C = \Delta C + C_0$ and $T = \Delta T + T_0$ are uniform moisture and temperature changes; C_0 and T_0 are reference moisture and temperature.

The classical and nonclassical boundary conditions can be obtained in the derivation process when using the integrations by parts. Thus, we obtain classical boundary conditions at $x = 0$ or a and $y = 0$ or b as

$$\begin{aligned} & \text{Specify } w_b \text{ or} \left(\frac{\partial M_{xx}^b}{\partial x} + \frac{\partial M_{xy}^b}{\partial y} \right) n_x + \left(\frac{\partial M_{yy}^b}{\partial y} + \frac{\partial M_{xy}^b}{\partial x} \right) n_y = 0 \\ & \text{Specify } \frac{\partial w_b}{\partial n} \text{ or } M_{xx}^b n_x^2 + n_x n_y M_{xy}^b + M_{yy}^b n_y^2 = 0 \end{aligned} \tag{22}$$

where $\frac{\partial()}{\partial n} = n_x \frac{\partial()}{\partial x} + n_y \frac{\partial()}{\partial y}$; n_x and n_y are the x and y components of the unit normal vector on the nanoplate boundaries, respectively and the nonclassical boundary conditions are

$$\begin{aligned} & \text{Specify } \frac{\partial^2 w_b}{\partial x^2} \text{ or } M_{xx}^{b(1)} = 0 \\ & \text{Specify } \frac{\partial^2 w_b}{\partial y^2} \text{ or } M_{yy}^{b(1)} = 0 \end{aligned} \tag{23}$$

Based on the NSGT, the constitutive relations of presented FG nanofilm can be stated as

$$\begin{aligned} & (1 - \mu\nabla^2) \begin{Bmatrix} \sigma_x \\ \sigma_y \\ \sigma_{xy} \\ \sigma_{yz} \\ \sigma_{xz} \end{Bmatrix} \\ & = \frac{E(z)}{1 - v^2} (1 - \lambda\nabla^2) \begin{pmatrix} 1 & v & 0 & 0 & 0 \\ v & 1 & 0 & 0 & 0 \\ 0 & 0 & (1-v)/2 & 0 & 0 \\ 0 & 0 & 0 & (1-v)/2 & 0 \\ 0 & 0 & 0 & 0 & (1-v)/2 \end{pmatrix} \\ & \times \begin{Bmatrix} \varepsilon_x - \gamma\Delta T - \beta\Delta C \\ \varepsilon_y - \gamma\Delta T - \beta\Delta C \\ \gamma_{xy} \\ \gamma_{yz} \\ \gamma_{xz} \end{Bmatrix} \end{aligned} \tag{24}$$

Integrating equation (24) over the plate's cross-sectional area, one can obtain the force-strain and the moment-strain of the nonlocal FG plates can be obtained as follows

$$\begin{aligned} & (1 - \mu\nabla^2) \begin{Bmatrix} N_x \\ N_y \\ N_{xy} \end{Bmatrix} = A(1 - \lambda\nabla^2) \begin{pmatrix} 1 & v & 0 \\ v & 1 & 0 \\ 0 & 0 & (1-v)/2 \end{pmatrix} \\ & \times \begin{Bmatrix} \frac{\partial u}{\partial x} \\ \frac{\partial v}{\partial y} \\ \frac{\partial u}{\partial y} + \frac{\partial v}{\partial x} \end{Bmatrix} \end{aligned} \tag{25}$$

$$(1-\mu\nabla^2)\begin{Bmatrix} M_x^b \\ M_y^b \\ M_{xy}^b \end{Bmatrix} = D(1-\lambda\nabla^2) \times \begin{pmatrix} 1 & v & 0 \\ v & 1 & 0 \\ 0 & 0 & (1-v)/2 \end{pmatrix} \begin{Bmatrix} -\frac{\partial^2 w}{\partial x^2} \\ -\frac{\partial^2 w}{\partial y^2} \\ -2\frac{\partial^2 w}{\partial x \partial y} \end{Bmatrix} \tag{26}$$

in which

$$A = \int_{-h/2}^{h/2} \frac{E(z)}{1-v^2} dz, \quad D = \int_{-h/2}^{h/2} \frac{E(z)(z-z^*)^2}{1-v^2} dz \tag{27}$$

The governing equations in terms of the displacements for a NSGT nanofilm can be derived by substituting equations (25) and (26), into equations (18) to (20) as follows

$$\begin{aligned} &A(1-\lambda\nabla^2)\left(\frac{\partial^2 u}{\partial x^2} + \frac{1-v}{2}\frac{\partial^2 u}{\partial y^2} + \frac{1+v}{2}\frac{\partial^2 v}{\partial x \partial y}\right) \\ &+ (1-\mu\nabla^2)\left(-I_0\frac{\partial^2 u}{\partial t^2} + I_1\frac{\partial^3 w}{\partial x \partial t^2}\right) = 0 \end{aligned} \tag{28}$$

$$\begin{aligned} &A(1-\lambda\nabla^2)\left(\frac{\partial^2 v}{\partial y^2} + \frac{1-v}{2}\frac{\partial^2 v}{\partial x^2} + \frac{1+v}{2}\frac{\partial^2 u}{\partial x \partial y}\right) \\ &+ (1-\mu\nabla^2)\left(-I_0\frac{\partial^2 v}{\partial t^2} + I_1\frac{\partial^3 w}{\partial y \partial t^2}\right) = 0 \end{aligned} \tag{29}$$

$$\begin{aligned} &-D(1-\lambda\nabla^2)\left(\frac{\partial^4 w}{\partial x^4} + 2\frac{\partial^4 w}{\partial x^2 \partial y^2} + \frac{\partial^4 w}{\partial y^4}\right) \\ &+ (1-\mu\nabla^2)\left(-I_0\frac{\partial^2 w}{\partial t^2} - I_1\left(\frac{\partial^3 u}{\partial x \partial t^2} + \frac{\partial^3 v}{\partial y \partial t^2}\right) \right. \\ &\left. + I_2\nabla^2\left(\frac{\partial^2 w}{\partial t^2}\right) - (N^T + N^H)\nabla^2 w - k_w w + k_P \nabla^2 w\right) = 0 \end{aligned} \tag{30}$$

Solution procedure

In this section, Galerkin's method is implemented to solve the governing equations of nonlocal strain gradient based FG nanofilms. Thus, the displacement field can be calculated as

$$u = \sum_{m=1}^{\infty}\sum_{n=1}^{\infty} U_{mn} \frac{\partial X_m(x)}{\partial x} Y_n(y) e^{i\omega_n t} \tag{31}$$

$$v = \sum_{m=1}^{\infty}\sum_{n=1}^{\infty} V_{mn} X_m(x) \frac{\partial Y_n(y)}{\partial y} e^{i\omega_n t} \tag{32}$$

$$w = \sum_{m=1}^{\infty}\sum_{n=1}^{\infty} W_{mn} X_m(x) Y_n(y) e^{i\omega_n t} \tag{33}$$

where (U_{mn}, V_{mn}, W_{mn}) are the unknown coefficients and the functions X_m and Y_n satisfy the boundary conditions. The classical and nonclassical boundary conditions based on the present plate model are

$$\begin{aligned} &w = 0, \\ &\frac{\partial^2 w}{\partial x^2} = \frac{\partial^2 w}{\partial y^2} = 0 \\ &\frac{\partial^4 w}{\partial x^4} = \frac{\partial^4 w}{\partial y^4} = 0 \end{aligned} \tag{34}$$

By substituting equations (31) to (33) into equations (28) to (30), and using the Galerkin's method, one obtains

$$[M]\{\ddot{\Lambda}\} + [[K] + N_0(t)[G]]\{\Lambda\} = 0 \tag{35}$$

where their components are presented in the Appendix. Also, [**M**], [**K**], and [**G**] denote the mass, stiffness, and geometric stiffness matrices, respectively, and $\{\Lambda\}$ is the displacement vector ($\{\Lambda\} = \{\mathrm{U_{mn}, V_{mn}, W_{mn}}\}$).

Considering periodic axial excitation compressive load $N_0(t) = -[\alpha + \beta\cos(\varpi t)]N_{cr}$, which consists of static and dynamical components, the governing equation can be expressed by

$$[M]\{\ddot{\Lambda}\} + [[K] - \{\alpha + \beta\cos(\varpi t)\}N_{cr}[G]]\{\Lambda\} = 0 \tag{36}$$

where ϖ and N_{cr} denote excitation frequency and buckling load respectively; α and β denote the static and dynamic load factors respectively. To calculate the dimensionless excitation frequency, the following relation is adopted

$$\Omega = \varpi a\sqrt{\frac{\rho_c}{\mathrm{E}_c}} \tag{37}$$

The instability boundaries considering periodic coefficients of the Mathieu–Hill type can be formed by periodic T_0 and $2T_0$ in which $T_0 = 2\pi/\varpi$. It is reported that the boundaries of instability regions with period T_0 are less important compared to those with period $2T_0$. The solution with respect to period $2T_0$ can be obtained by the following equation

$$[[K] - N_{cr}\{\alpha \pm 0.5\beta\}[G] - 0.25\varpi[M]]\{\Lambda\} = 0 \tag{38}$$

The nontrivial solution of equation (38) gives

$$\det\begin{vmatrix} \begin{Bmatrix} [\bar{K}] - (0.5\beta)N_{cr}[G] \\ -(0.25\varpi)[M] \end{Bmatrix} & 0 \\ 0 & \begin{Bmatrix} [\bar{K}] + (0.5\beta)N_{cr}[G] \\ -(0.25\varpi)[M] \end{Bmatrix} \end{vmatrix} = 0 \tag{39}$$

Table 1. Comparison of the nondimensional fundamental natural frequency FG nanofilms with simply-supported boundary conditions ($p = 5$).

		$a/b = 1$		$a/b = 2$	
a/h	μ	Natarajan et al.[36]	Present	Natarajan et al.[36]	Present
10	0	0.0441	0.0439	0.1055	0.1045
	1	0.0403	0.0401	0.0863	0.0856
	2	0.0374	0.0372	0.0748	0.0742
	4	0.0330	0.0329	0.0612	0.0608
20	0	0.0113	0.0112	0.0279	0.0277
	1	0.0103	0.0102	0.0229	0.0227
	2	0.0096	0.0095	0.0198	0.0197
	4	0.0085	0.0084	0.0162	0.0161

in which $[\bar{K}] = [K] - \alpha N_{cr}[G]$. For a given value of α, the plots of eigenfrequency Ω with respect to β provide stability regions of the nonlocal FGM nanoplates. Also, non-dimensional parameters are defined as

$$K_w = \frac{k_w a^4}{D_c}, \quad K_p = \frac{k_p a^2}{D_c}, \quad D_c = \frac{E_c h^3}{12(1 - v_c^2)} \tag{40}$$

Finally, setting the coefficient matrix to zero gives the natural frequencies. The function X_m for simply-supported boundary conditions is defined by

$$X_m(x) = \sin(\lambda_m x)$$
$$\lambda_m = \frac{m\pi}{a} \tag{41}$$

The function Y_n can be obtained by replacing x, m, and a, respectively by y, n, and b.

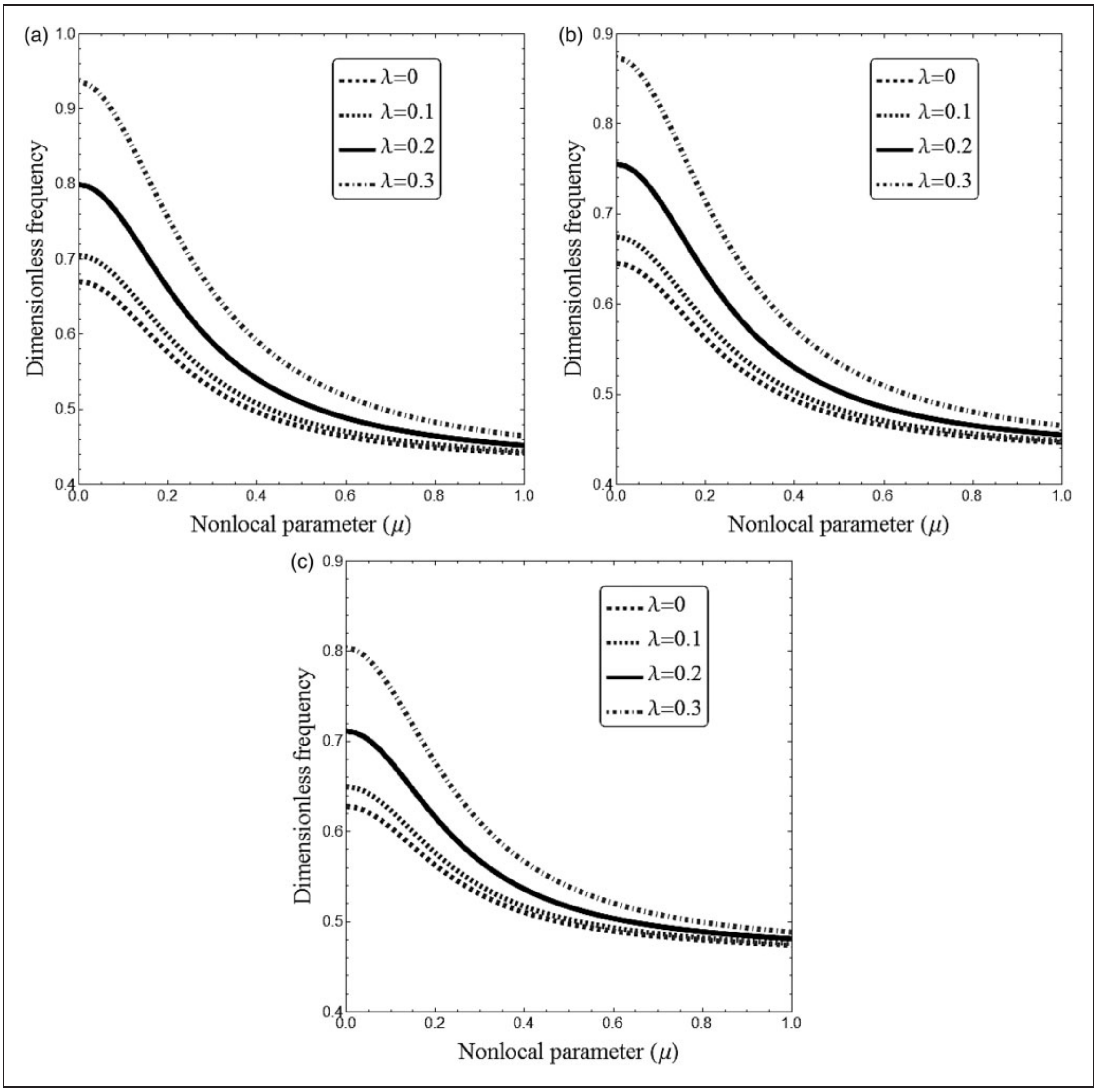

Figure 2. Variation of dimensionless frequency of porous nanofilms versus nonlocal parameter for different strain gradient parameters ($a/h = 20$, $\Delta T = 50$, $\Delta C = 1\%$, $K_w = 25$, $K_p = 10$): (a) $p = 0.5$; (b) $p = 1$; (c) $p = 5$.

Numerical results and discussions

This section is concerned with the dynamic modeling and analysis of harmonically loaded porous FG nanofilms in hygro-thermal environments according to the nonlocal strain gradient theory. Therefore, both nonlocality of stress field as well as strain gradients are considered. The correctness of the obtained vibration frequencies via present plate model are verified with those of first-order shear deformation theory obtained by Natarajan et al.[36] using finite element method and the results are tabulated in Table 1. It is noticeable that presented Galerkin's solution can accurately predict vibrational behavior of FG nanoplates. The length of nanoplate is assumed as $a = 50\,\mathrm{nm}$. Also, material properties of nanoplate (alumina and aluminum) are considered as

- $E_c = 380\,\mathrm{Gpa}$, $\rho_c = 3800\,\mathrm{kg/m^3}$, $v_c = 0.3$, $\alpha_c = 7 \times 10^{-6} {}^\circ\mathrm{C}^{-1}$, $\beta_c = 0.001\ (\mathrm{wt\%H_2O})^{-1}$
- $E_m = 70\,\mathrm{Gpa}$, $\rho_m = 2707\,\mathrm{kg/m^3}$, $v_m = 0.3$, $\alpha_m = 23 \times 10^{-6} {}^\circ\mathrm{C}^{-1}$, $\beta_m = 0.44\ (\mathrm{wt\%H_2O})^{-1}$

A study on the variation of natural frequency of hygro-thermally affected FG nanofilms with respect to nonlocal and strain gradient parameters is conducted in Figure 2 when $a/h = 20$, $\Delta T = 50$, $\Delta C = 1\%$, $\xi = 0.05$, $K_w = 25$, and $K_p = 10$. It is clear that natural frequency of FG nanofilm reduces with the increase of nonlocal parameter for every value of strain gradient parameter. But, vibration frequency increases at a fixed nonlocal parameter and inhomogeneity index. Due to the lack of a strain gradient parameter in previous vibration analyses of nanofilms, only the softening effect due to nonlocality was concluded. Therefore, the material instability and heterogeneous deformation due to strain gradient could not be considered within the framework of the nonlocal elasticity theory.

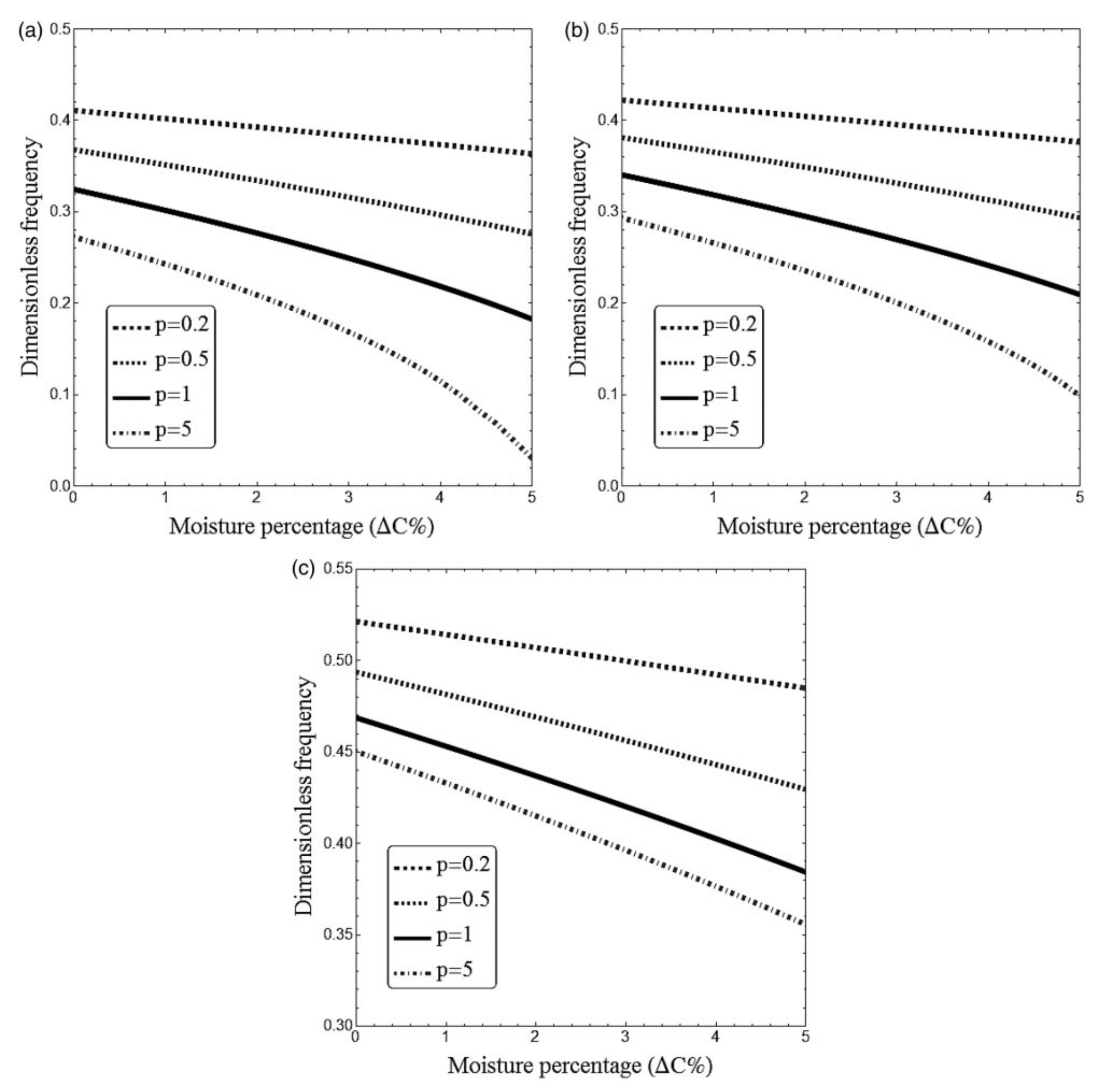

Figure 3. Variation of dimensionless frequency of porous nanoplates versus moisture percentage for various power-law indices ($a/h = 20$, $\Delta T = 100$, $\mu = 0.2$, $\lambda = 0.1$): (a) $K_w = 0$, $K_p = 0$; (b) $K_w = 10$, $K_p = 0$; (c) $K_w = 10$, $K_p = 5$.

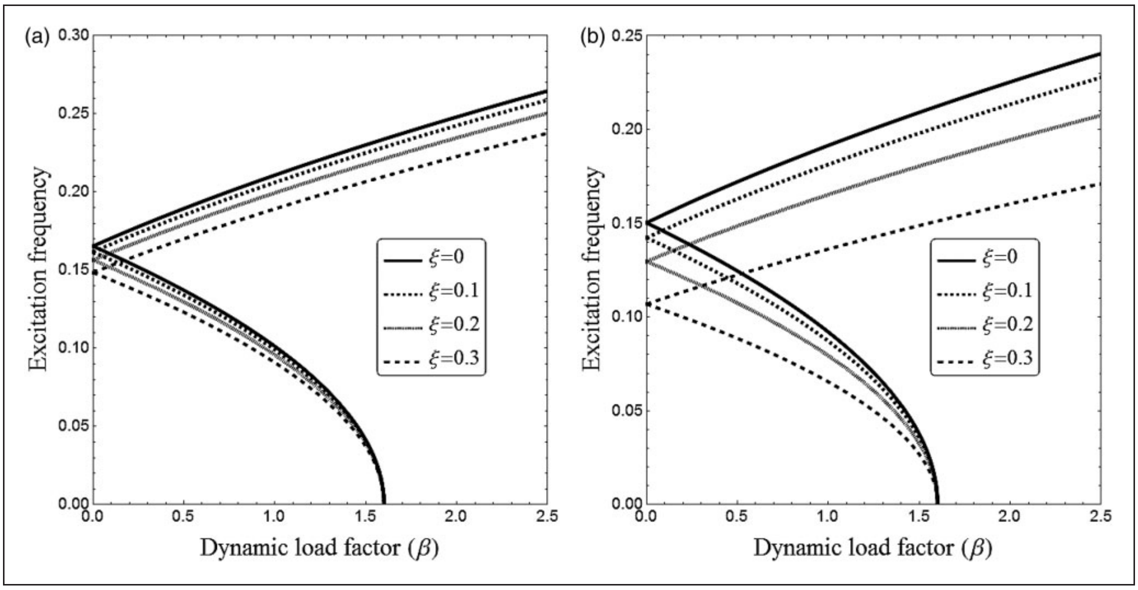

Figure 4. Dimensionless frequency of the nanoplate versus dynamic load factor for different gradient index and porosity volume fractions ($a/h = 20$, $\alpha = 0.2$, $K_w = 0$, $K_p = 0$): (a) $p = 1$; (b) $p = 2$.

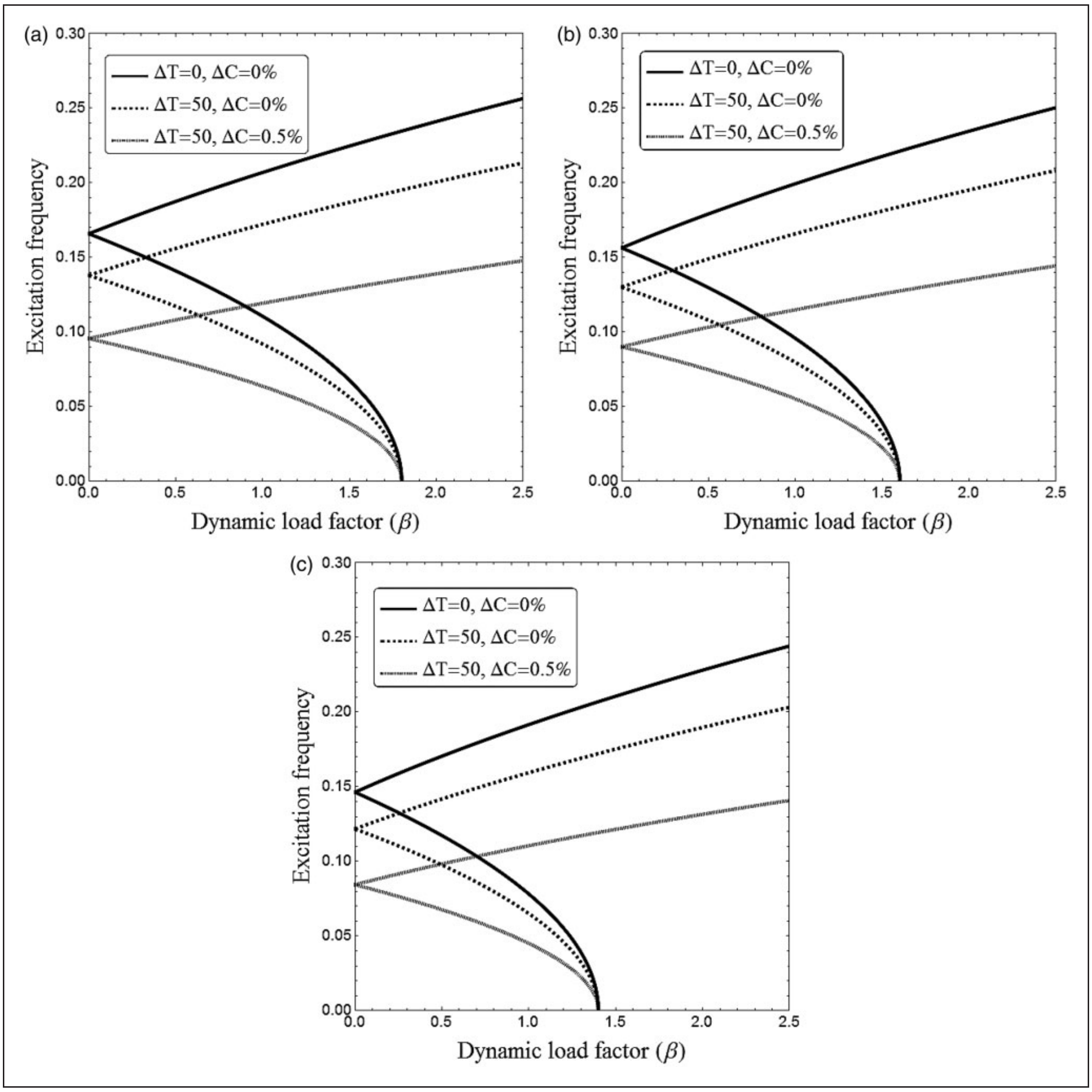

Figure 5. Dimensionless frequency of the nanofilm versus dynamic load factor for different moisture percentage rises and static load factors ($a/h = 20$, $p = 1$, $\xi = 0.2$, $K_w = 0$, $K_p = 0$, $\mu = 0.2$, $\lambda = 0.1$): (a) $\alpha = 0.1$; (b) $\alpha = 0.2$; (c) $\alpha = 0.3$.

In Figure 3, dimensionless frequency of FG nanofilm with respect to moisture change is plotted for a variety of material gradient index and elastic substrate coefficients. It is well-known that an increment in moisture value results in lower stiffness of nanofilm. Accordingly, magnitude of vibration frequency diminishes with the increase of moisture value. However, an influence of moisture change relies on the magnitude of material gradient index. Actually, a FG nanofilm is more affected by the moisture change at larger magnitudes of material gradient index because of higher portion of metal phase. Actually, moisture expansion coefficient of ceramic phase is significantly smaller than that of metal phase. Thus, higher portion of ceramic phase yields lower impact of moisture on the nanofilm. One can also see that elastic substrate can enhance the mechanical performance of FG nanofilm leading to larger vibration frequencies. In fact, both Winkler and Pasternak coefficients of elastic substrate yields bigger frequencies regardless of the moisture change.

Dynamic frequency of a periodically loaded FG nanofilm with respect to dynamic load parameter is plotted in Figure 4 for different porosity volume fractions when $\mu = 0.2$, $\alpha = 0.2$, $K_w = 0$, and $K_p = 0$. It is well-known that the dispersion of porosities in the material structures degrades the nanofilm stiffness leading to lower vibration frequencies. However, the instability region becomes smaller with the increase of porosity volume fraction. In other words, stability boundary is wider at lower values of porosity volume fraction. Therefore, porosities inside the material have a major role on unstable region and should be considered in dynamic analysis of nanofilms.

In Figure 5, impacts of temperature, moisture, and static load parameter on stability regions of harmonically loaded porous FG nanofilms are presented when $a/h = 20$, $p = 1$, $\xi = 0.2$, $K_w = 0$, $K_p = 0$, $\mu = 0.2$, and $\lambda = 0.1$. It can be observed in the figure that when the moisture percentage increases, the dynamic buckling boundaries are degraded. It means that the parametric instability can be enhanced by the moisture change. However, the starting point ($\beta = 0$) is reduced with the increase of moisture percentage. The reason is that the existence of humidity field diminishes the bending rigidity of the FG nanofilms leading to the reduction in the frequencies. According to this figure, when the static load factor rises, the boundaries of dynamic instability region reduce at a fixed nonlocal parameter. This is due to the fact that compressive static load degrades the flexibility of the FG nanofilm, and leads to smaller excitation frequencies. One can see that the instability region of FGM nanofilms becomes closer to the origin by increasing the magnitude of static load factor.

Figure 6 examines the variation of dimensionless frequency of the nanofilm versus dynamic load factor for different side-to-thickness ratios at $p = 1$, $\xi = 0.2$, $K_w = 10$, $K_p = 5$, $\mu = 0.2$, $\lambda = 0.1$, $\Delta T = 50$, and $\Delta C = 0.5\%$. It is well known that the nanofilm becomes more flexible at larger values of side-to-thickness ratio. It is observed that stability boundaries are wider at smaller values of side-to-thickness ratio. Also, starting point ($\beta = 0$) or natural frequency of porous FG nanofilm reduces with the increase of side-to-thickness ratio.

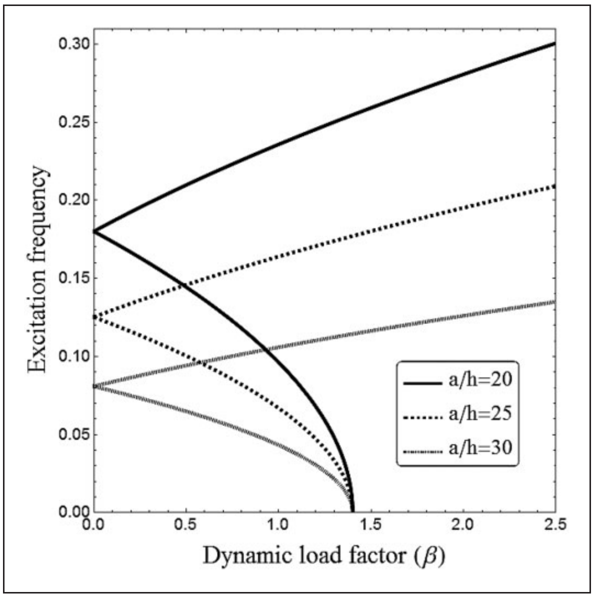

Figure 6. Dimensionless frequency of the nanofilm versus dynamic load factor for different side-to-thickness ratios ($p = 1$, $\xi = 0.2$, $K_w = 10$, $K_p = 5$, $\mu = 0.2$, $\lambda = 0.1$, $\Delta T = 50$, $\Delta C = 0.5\%$).

Conclusions

This paper was concerned with the dynamic modeling and analysis of harmonically loaded porous FG nanofilms in hygro-thermal environments according to the nonlocal strain gradient theory. Therefore, both nonlocality of stress field as well as strain gradients were considered. The classical plate model was employed for modeling of FG nanofilm. Nonlocal parameter gave smaller frequencies, while strain gradient parameter gave larger frequencies for FG nanofilm. A significant change was observed in the stability boundaries of FG nanofilm due to the variation of moisture and temperature. However, the effect of moisture change on the dynamic behavior of FG nanofilm depends on the value of material gradient index. Also, increasing porosity volume fraction led to lower stiffness and vibration frequency of FG nanofilm.

Declaration of Conflicting Interests

The author(s) declared no potential conflicts of interest with respect to the research, authorship, and/or publication of this article.

Funding

The author(s) received no financial support for the research, authorship, and/or publication of this article.